arXiv:1303.3831v2 [cond-mat.mtrl-sci] 9 Apr 2013

# X-ray induced trap states in the organic semiconductor Rubrene

Tobias Morf,* Simon Haas,† Tino Zimmerling,‡ and Bertram Batlogg§
*Laboratory for Solid State Physics, ETH Zurich, 8093 Zurich, Switzerland*

(Dated: April 10, 2013)

In view of applications in X-ray detectors and field-effect transistors it is important to enhance to understanding of formation and microscopic origin of localised states in organic semiconductors. In a controlled irradiation experiment, the formation of trap states in the prototypical organic semiconductor Rubrene is studied quantitatively for doses up to 82 Gy ($= \mathrm{J\,kg^{-1}}$). About 100 electronic trap states, located around 0.3 eV above the valence band, are created by each absorbed photon, equivalent to $10^{14}$ new states per Gray. Compared to ion irradiation, X-rays generate 100 to 1000 times more trap states per primary interaction event. Thermal annealing is shown to reduce these traps.

PACS numbers: 71.20.Rv 72.80.Le
Keywords: CHARGE-LIMITED CURRENT; SINGLE-CRYSTAL; TRANSPORT; MOBILITY; ENERGY; X-RAY; TRAP STATE; ORGANIC SEMICONDUCTOR

Owing to the envisioned application in X-ray scintillators, the radiation damage inflicted to organic crystals and the related degradation of optical properties was intensely studied in the 1970s mostly on anthracene (e.g. [1–4]). In the meantime, inorganic scintillators have found widespread application, yet organic materials are considered anew for direct X-ray detection through the photoconductivity effect [5, 6]. Due to low-cost, large-area processing, organic materials would allow the production of large-scale integrated X-ray imaging panels at a fraction of todays costs [6]. For those applications, it will be of central importance to assess the radiation damage and whether those defects can be healed by thermal annealing.

Furthermore, an unexpected positive influence of X-ray radiation in electron-beam evaporation processes on the magnetotransport in organic materials has been reported [7]. These effects, together with the commonly known adverse influence of traps on charge transport [8] as well as spin diffusion length [7], are a strong motivation to further investigate the defects arising from X-ray radiation.

In this study we address the formation of electronic trap states upon X-ray irradiation in Rubrene single crystals, a grain boundary free model material. The simultaneous measurement of up to four sites on the same crystal — called channels — provides verifiable results and the shielding of some of these channels during irradiation allows the reliable attribution of the observed effects to the actual X-ray irradiation. Furthermore, this sample arrangement (c.f. fig. 1) enables checking of reproducibility and device stability.

The crystals' spectral density of trap states (DOS) is determined without any *a priori* assumptions by measuring current voltage characteristics at different temperatures and applying temperature-dependent space-charge limited current spectroscopy (TD-SCLC). The basic concept of SCLC is electrical transport by thermally excited charge carriers. Due to the Fermi-Dirac statistics this excitation from localised traps to delocalised, conducting states takes place in a small energy window. If the Fermi energy $E_F$ is shifted with increasing voltage additional space charge is injected. The trap DOS is deconvoluted from this differential increment. The energy scale is given by the thermal activation energy at a given voltage corrected by the statistical shift, which accounts for the asymmetry of the DOS around $E_F$. The full procedure is formally discussed in references 9–13 and numerically implemented using cubic smoothing splines [14].

Rubrene crystals were grown by physical vapour transport in high purity argon flow and are platelet-like with the surface perpendicular to the 26.86 Å long crystallographic $a$ axis [15–17] which is also the direction of current flow in our experiments. With a modified 'flip-

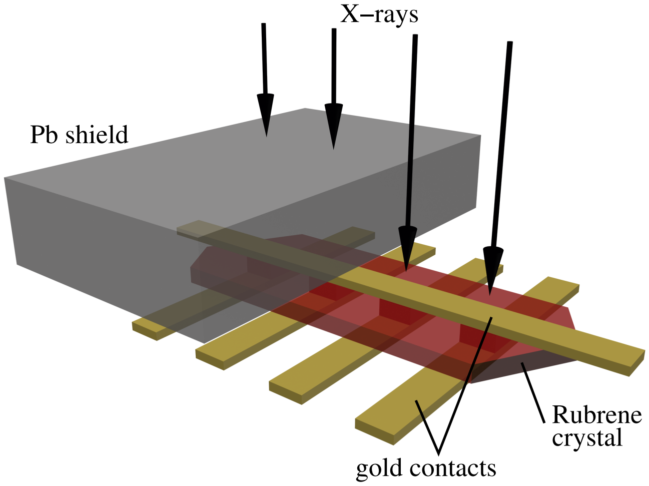

FIG. 1: (Colour online) Schematic of the sample layout for SCLC measurements and X-ray irradiation. The Rubrene crystal is laminated onto the prefabricated bottom contacts, then the top electrode is evaporated. The lead shield screens part of the crystal from X-rays, thus allowing direct comparison of irradiated to unirradiated crystal sites.

crystal' technique [18] the crystals were laminated onto prefabricated gold electrodes. For the vacuum evaporation of the top electrode, the samples were slightly cooled in order to minimise the thermal load on the crystals. The resulting sample layout is schematically shown in fig. 1.

The electric SCLC measurements of the crystals were performed in darkness in the inert helium atmosphere of a cryostat. Charge carrier injection from the laminated bottom electrodes turned out to be more efficient than from the deposited top contacts and thus the polarity for all measurements was chosen accordingly. Current and power limits prevent crystal damage [19] or local heating.

After transferring the samples to an argon filled tube the crystals were exposed to X-rays in the beam of a diffractometer. The lateral intensity distribution (beam shape) of the monochromatic CuK$\alpha$ beam (8 keV) was measured with the diffractometer's image-plate detector and multiple Zirconium attenuators and extrapolated to zero shielding. For the calibration of the intensity in absolute units, a calibrated instrument was required. While dosimeters for therapeutical and radiological applications are usually calibrated for energies much higher than 8 keV, a suitable instrument was kindly provided by the University Hospital of Zurich. The beam's peak intensity was calculated as $3\,\mu\mathrm{W\,cm^{-2}}$ corresponding to a photon flux of $2 \times 10^9\,\mathrm{s^{-1}\,cm^{-2}}$. Approximating Rubrene in first order as stoichiometric 42:28 mixture of carbon and hydrogen and assuming the crystal to be centred at maximum intensity, the absorbed dose during one hour of exposure was $(41 \pm 9)$ Gy ($= \mathrm{J\,kg^{-1}}$) [20]. For comparison, a single computed tomography (CT) scan accounts for up to 10 mGy [21], typical radiotherapy doses are some 10 Gy [22] and the accumulated lifetime dose of X-ray imaging sensors is a few 100 Gy [6].

After first measuring the trap DOS of the pristine crystals, the samples were aligned in the beam with fluorescent marks as reference and irradiated. During irradiation, two out of four channels were shielded by a 0.1 mm lead foil thus providing reference data on the same crystal. After each hour of irradiation, the samples were measured and the trap DOS calculated. These repeated measurements required the crystals to be stable over multiple thermal cycles between 300 K and 100 K.

The current-voltage characteristics at two selected temperatures are shown in the top panel of Fig. 2. The formation of trap states is seen at once in these data: traps capture injected charge and thus reduce the current levels. Such a reduction is not observed in shielded parts of the crystal (represented by grey lines). The current activation energy $E_A^{\mathrm{SCL}}$ at fixed voltage shown in the bottom panel of Fig. 2 reveals that above $\approx 0.2$ V charge carriers are efficiently injected and the Fermi energy shifts towards the valence band edge with higher voltage. The progressive flattening of the slope below 0.35 eV indicates an increased DOS after exposure to X-rays which is again confirmed by the unirradiated reference remaining unchanged.

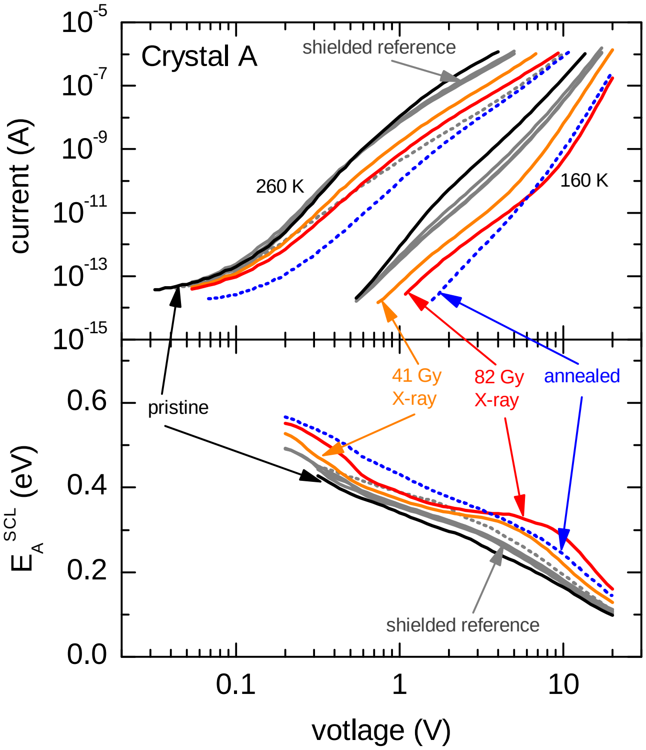

FIG. 2: (Colour online) **Top panel:** Current-voltage characteristics of a typical Rubrene single crystal device. The linear, Ohmic regime at low voltages is followed by the filling of traps and a steep increase in current. In this regime the current is reduced with increasing irradiation time due to a higher density of trap states (unirradiated: black; 41 Gy: orange; 82 Gy: red; annealed: blue; shielded parts: grey). **Bottom panel:** Activation energy-voltage mapping for the same sample as above. The increasing trap DOS after one and two hours of X-ray irradiation is seen as a flattening of the slope at 0.35 eV.

The density of states extracted from the data in Fig. 2 (crystal thickness $0.8\,\mu$m, cross-section $1.4 \times 10^{-5}\,\mathrm{cm^2}$) and from a second sample are shown in Fig. 3. The unirradiated channels do not show any significant change in the trap DOS compared to the pristine state. This is direct evidence for X-ray induced trap states and also reflects the stability and reproducibility of sample handling and measurement.

In the exposed channels, the trap DOS increases by up to $8 \times 10^{16}\,\mathrm{cm^{-3}\,eV^{-1}}$ (fig. 3, crysal B) in a narrow energy range peaked around 0.3 eV. The area under this peak yields the total trap density of $\sim 3 \times 10^{15}\,\mathrm{cm^{-3}}$ traps generated during one hour of X-ray irradiation. After the second hour of irradiation, the induced trap density has doubled within experimental uncertainty.

The hourly dose of 41 Gy corresponds to $4 \times 10^{13}\,\mathrm{cm^{-3}}$ absorbed photons (0.05 % of incident photons for a $1\,\mu$m thick crystal). Every one of these *primary events* will

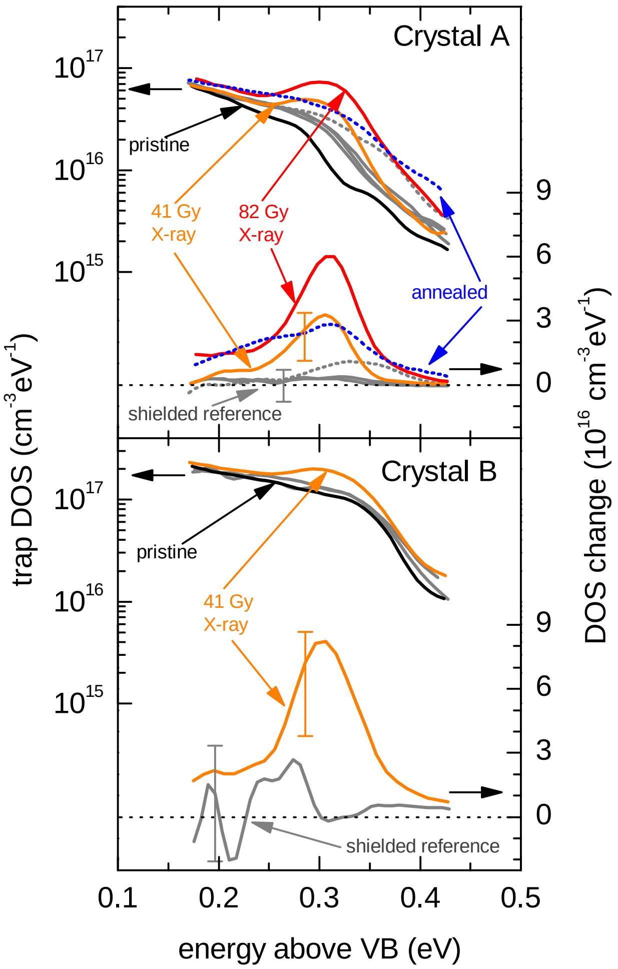

FIG. 3: (Colour online) Trap density of states and its change upon X-ray irradiation in Rubrene single crystals. The valence band edge (VB) is chosen as the energy reference point. Crystal A in the top panel is the same device as shown in Fig. 2 and the symbols and lines are used in the same sense. The distinct increase peaked at 0.3 eV is attributed to X-ray induced defects since the shielded parts (grey) do not show any significant changes. Annealing of the sample suggests that structural defects significantly contribute to the total trap state density.

deposit the full photon energy of 8 keV and causes a cascade of secondary events which in turn create numerous microscopic defects. This response is in distinct contrast to the energy deposition and trap generation by ions [23].

To compare X-ray and ion irradiation it is appropriate to consider the microscopic interaction mechanism as sketched in the insets of fig. 4. On its way through a 1 µm thick crystal, every proton of 1 MeV experiences approximately 14 *primary interactions*, each time transfering ≈ 2.3 keV to the crystal's electronic system [24] (energy transfer to atom displacements is negligible [32]).

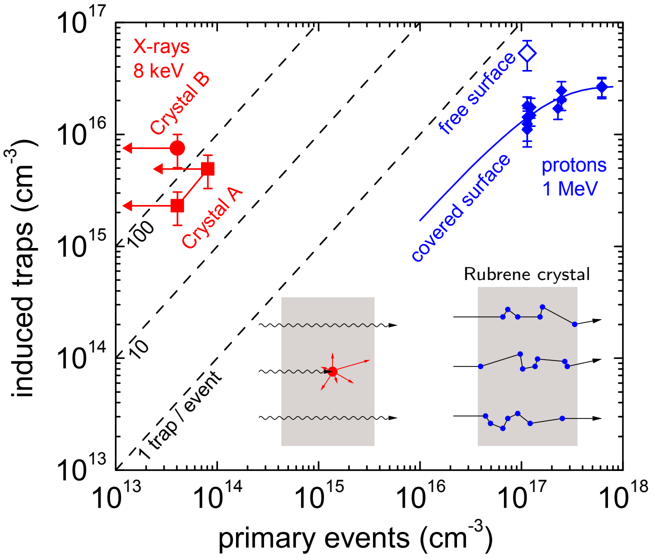

FIG. 4: (Colour online) Trap density in Rubrene crystals irradiated by X-rays (red) or protons (blue, [23]). For each primary interaction event, protons create ∼ 0.2 traps to 0.5 traps, while X-rays produce ∼ $10^2$ traps. The 100 to 1000 times higher trap creation efficiency of X-rays is attributed to secondary events. Trap creation by ions in covered crystals saturates due to re-attachement of hydrogen. The insets schematically show the energy deposition processes. An X-ray photon will either pass the crystal undisturbed or deposit its full energy in a single event creating numerous secondary events. On the other hand, every ion will experience several interactions with (mainly) target electrons every time depositing a fraction of its initial energy.

In fig. 4 the density of radiation-induced traps is plotted as a function of primary events. Note that the primary event counts of the X-ray datapoints are an upper limit based on the assumption that the samples were centred at peak intensity. For quantitative comparison, the ion irradiated crystal with an open surface (open symbol) is considered since the same layout was used for the X-ray irradiated samples. Solid symbols are data from covered surfaces saturating at high dose due to re-attachement of hydrogen knocked off in a previous event. For each primary interaction event, protons create ∼ 0.5 traps, while X-rays produce ∼ $10^2$ traps. A central result of this study is: per primary interaction event, X-rays are found to be 100 to 1000 times more effective than ions in trap generation. This is attributed to the shower of secondary events following every photon absorption.

In order to further elucidate the origin of radiation induced trap states, Crystal A in fig. 3 has been annealed for 12 h at 350 K. This removed approximately 40 % of the defects and doubled the width of the spectral distribution. This annealing may suggest that some of the produced defects are of structural nature and it is consistent with previous observations in anthracene crystals [3, 25, 26]. Displacement of molecules by photons or secondary electrons/ions has to be considered a possible process for the creation of trap states due to the weak vander-Waals bonding between organic molecules. This is in distinct contrast to silicon which has a displacement energy of 21 eV [27]. Consequently, no defects are observed in amorphous silicon under X-ray radiation [19, 28]. In organic materials however, imperfections in the lattice geometry such as stacking faults, dislocations or local disorder due to chemical impurities alter the intermolecular distance which in turn changes the molecule's polarisation energy and thus results in the formation of new electronic states.

Chemical defects will introduce their own, localised states and may also cause a local perturbation of the extended states if they are charged or polarised. There are several proposed processes for introducing chemical defects. An X-ray photon absorbed in the crystal will likely break bonds of Rubrene molecules [29] thus leaving new chemical species in the bulk Rubrene. Molecules with such dangling bonds may then cross-link again [30]. A detached Hydrogen atom may be re-absorbed in a different place [23], even at another Hydrogen bond [31]. I will be interesting to know to what degree thermal annealing will promote these processes. If impurities such as residual water or oxygen are already present in the crystal, they might get activated and cause further damage to the host material [26].

Either effects — structural or chemical — will cause a modification of the local geometric arrangement and thus a shift of the energy levels of the intact molecules due to a modified polarisation energy. In addition, the energy of the molecular levels will be affected by the proximity of a detached ion.

In conclusion, space-charge limited current spectroscopy is applied to study the formation of bulk trap states in Rubrene single crystals under 8 keV X-ray irradiation. New trap states are generated around 0.3 eV from the valence band edge with an efficiency on the order of 100 traps per absorbed 8 keV photon. Thermal annealing of irradiated samples significantly reduces the trap density. These observations enhance the understanding of trap state formation and annealing in organic semiconductors [8] especially in light of applications in X-ray imaging.

The authors wish to thank Carlo Bernasconi from the Laboratory of Crystallography, ETH Zurich for access to the X-ray diffractometer. Stephan Klöck and Jérôme Krayenbühl from University Hospital Zurich are greatfully acknowledged for their help in measuring the X-ray intensity and Kurt Mattenberger for support with various technical issues.

---

[*] tmorf@phys.ethz.ch

[†] s.haas@alumni.ethz.ch

[‡] tino.zimmerling@phys.ethz.ch

[§] batlogg@phys.ethz.ch

[1] S. Weisz, A. Cobas, P. E. Richardson, H. H. Szmant, and S. Trester, J. Chem. Phys. **44**, 1364 (1966).

[2] J. Birks, Proc. Phys. Soc. A **64**, 874 (1951).

[3] K. Yokoi and Y. Ohba, Chem. Phys. Lett. **56**, 560 (1978).

[4] N. Shiomi, J. Phys. Soc. Jpn. **23**, 1177 (1967).

[5] C. R. Newman, H. Sirringhaus, J. C. Blakesley, and R. Speller, Appl. Phys. Lett. **91**, 142105 (2007).

[6] J. Blakesley, P. Keivanidis, M. Campoy-Quiles, C. Newman, Y. Jin, R. Speller, H. Sirringhaus, N. Greenham, J. Nelson, and P. Stavrinou, Nucl. Instrum. Methods Phys. Res., Sect. A **580**, 774 (2007).

[7] J. Rybicki, R. Lin, F. Wang, M. Wohlgenannt, C. He, T. Sanders, and Y. Suzuki, Phys. Rev. Le **109**, 076603 (2012).

[8] W. L. Kalb, S. Haas, C. Krellner, T. Mathis, and B. Batlogg, Phys. Rev. B **81**, 155315 (2010).

[9] O. Zmeškal, F. Schauer, and S. Nešpůrek, J. Phys. C: Solid State Phys. **18**, 1873 (1985).

[10] F. Schauer, S. Něspůrek, and O. Zmeškal, J. Phys. C: Solid State Phys. **19**, 7231 (1986).

[11] F. Schauer, S. Něspůrek, and H. Valerián, J. Appl. Phys. **80**, 880 (1996).

[12] F. Schauer, R. Novotny, and S. Nešpůrek, J. Appl. Phys. **81**, 1244 (1997).

[13] S. Nešpůrek, O. Zmeškal, and F. Schauer, Phys. Status Solidi A **85**, 619 (1984).

[14] C. de Boor, *A practical guide to splines*, vol. 27 of *Applied mathematical science* (Springer Verlag, New York, 1987).

[15] O. D. Jurchescu, A. Meetsma, and T. T. Palstra, Acta Crystallogr., Sect. B: Struct. Sci. **62**, 330 (2006).

[16] E. Menard, A. Marchenko, V. Podzorov, M. E. Gershenson, D. Fichou, and J. A. Rogers, Adv. Mater. **18**, 1552 (2006).

[17] T. Minato, H. Aoki, H. Fukidome, T. Wagner, and K. Itaya, Appl. Phys. Lett. **95**, 093302 (2009).

[18] J. Takeya, C. Goldmann, S. Haas, K. Pernstich, B. Ketterer, and B. Batlogg, J. Appl. Phys. **94**, 5800 (2003).

[19] J. Srour, J. Palko, D. Lo, S. Liu, R. Mueller, and J. Nocerino, IEEE T. Nucl. Sci. **56**, 3300 (2009).

[20] J. Hubbell and S. Seltzer, *Tables of x-ray mass attenuation coefficients and mass energy-absorption coefficients*, URL `http://physics.nist.gov/PhysRefData/XrayMassCoef/cover.html`.

[21] D. J. Brenner and E. J. Hall, N. Engl. J. Med. **357**, 2277 (2007).

[22] J. Krayenbühl, private communications.

[23] T. Zimmerling, K. Mattenberger, M. Döbeli, M. J. Simon, and B. Batlogg, Phys. Rev. B **85**, 134101 (2012).

[24] M. Pope and C. E. Swenberg, *Electronic processes in organic crystals and polymers* (Oxford University Press, 1999).

[25] G. Heppell and R. Hardwick, Trans. Faraday Soc. **63**, 2651 (1967).

[26] C. Zorn, Nucl. Phys. B, Proc. Suppl. **32**, 377 (1993).

[27] A. Akkerman, J. Barak, M. Chadwick, J. Levinson, M. Murat, and Y. Lifshitz, Radiat. Phys. Chem. **62**, 301 (2001).

[28] J. Srour, G. Vendura, D. Lo, C. Toporow, M. Dooley, R. Nakano, and E. King, IEEE T. Nucl. Sci. **45**, 2624 (1998).

[29] R. Barillon and T. Yamauchi, Nucl. Instrum. Methods Phys. Res., Sect. B **208**, 336 (2003).

[30] A. Quaranta, A. Vomiero, S. Carturan, G. Maggioni, and G. Della Mae, Synth. Met. **138**, 275 (2003).
[31] K. Nakagawa and N. Itoh, Chem. Phys. **16**, 461 (1976).
[32] Ion absorbtion was simulated using the same SRIM parameters as in ref. [23].